

# 000 PARALLEL PROMPTING: FAST LLM INFERENCE FOR 001 SHARED-CONTEXT, SHORT-TO-MODERATE OUTPUT 002

003 **Anonymous authors**  
004

005 Paper under double-blind review  
006

## 007 ABSTRACT 008

009 We introduce *Parallel Prompting*, a method for high-throughput, quality-preserving  
010 decoding of multiple large language model (LLM) queries that share a common  
011 prefix. Such shared-context structure arises naturally in applications including  
012 document question answering, few-shot learning, multi-user chat, and evaluation  
013 pipelines. Prior approaches either degrade generation quality by merging queries  
014 into a single prompt that the model cannot reliably disentangle or impose rigid  
015 batching and preallocated memory that limit practical deployment. Parallel Prompt-  
016 ing is a free lunch for batch prompting: it improves throughput and memory  
017 efficiency without requiring model retraining or sacrificing accuracy. The gains  
018 are most pronounced when prefix overlap is high and output lengths are short to  
019 moderate, with the relative advantage diminishing as unique suffixes grow longer.  
020 Our method executes a single pass over the shared context and decodes all con-  
021 tinuations in parallel through efficient matrix–matrix operations, while avoiding  
022 cross-query interference and supporting flexible batching across multiple sharing  
023 groups with dynamic, on-demand KV-cache management. This design enables  
024 high resource utilization during decoding without compromising output quality.  
025 Experiments on popular datasets with Llama 3-8B show up to a 4 $\times$  reduction  
026 in end-to-end latency relative to competitive baselines, with no loss in accuracy,  
027 demonstrating that Parallel Prompting complements existing batching strategies  
028 and expands the practical throughput of LLM-based systems.  
029

## 030 1 INTRODUCTION 031

032 Batch text generation is a standard paradigm for large language model (LLM) inference. In many  
033 practical scenarios, prompts within a batch often share a common prefix. This setting is prevalent  
034 in wide range of use-cases, such as document question answering, few-shot learning, multi-user  
035 chat, LLM-as-judges for model evaluation, and LLM-based verification for fact-checking. For  
036 instance, chatbots frequently serve diverse users using a shared system prompt, assistant models  
037 leverage few-shot exemplars for domain-specific tasks, and programming systems generate multiple  
038 candidate solutions to a single problem. As deployment of transformer-based LLMs continues to  
039 scale, harnessing these shared prefixes for efficiency becomes increasingly valuable.  
040

041 A growing body of work seeks to accelerate LLM inference by exploiting shared information across  
042 requests. Several systems (Zhu et al., 2024; Juravsky et al., 2024) reuse parts of the cache when  
043 different prompts begin with the same prefix, thereby avoiding redundant computation. While these  
044 approaches achieve meaningful speedups, they remain limited in important ways: some require rigid  
045 memory layouts, and others only handle batches in which all inputs share exactly the same prompt.  
046 Related methods (Kwon et al., 2023; Zheng et al., 2024; Gim et al., 2024) extend cache reuse further  
047 but still follow a fundamentally sequential decoding pattern, leaving substantial efficiency gains  
048 unrealized. Meanwhile, simple batch prompting strategies that merge multiple queries into a single  
049 prompt often degrade output quality because the model cannot reliably separate the different requests.  
050 These limitations highlight the need for a method that simultaneously avoids interference, supports  
051 flexible sharing groups, and fully exploits parallelism during decoding.  
052

053 In this paper, we propose **Parallel Prompting**, a method for efficiently decoding multiple queries with  
a shared prefix by processing them in parallel. The key insight is that we can independently encode  
each query with respect to the shared context using specialized attention masks, then generate outputs

054 in parallel during the decoding phase. This approach leverages efficient matrix-matrix operations on  
 055 modern GPUs to achieve significant speedups without compromising output quality. Critically, we  
 056 find that maximizing throughput requires carefully balancing two parameters: the batch size and the  
 057 degree of parallelism during decoding—the optimal point depends on hardware and model specifics.  
 058

059 To summarize, our work makes the following contributions:

060

- 061 • We propose a simple and effective method leveraging parallel prompting in LLM that allows  
 062 efficient batching of multiple LLM prompts which share a prefix.
- 063 • We conduct extensive experiments and show that our method can achieve improvements  
 064 in throughput and computational resource management over prior methods across a range  
 065 of workloads, although there are some workloads for which our proposed method is less  
 066 efficient than some prior methods.
- 067 • We show theoretically and experimentally that maximizing inference throughput for parallel  
 068 prompting requires a careful balance between attention parallelism and batch size.

069

| Prompt              |             | Generation                         |              |                   |
|---------------------|-------------|------------------------------------|--------------|-------------------|
| Generation Timestep |             | Batch Prompting (Cheng et al 2023) |              | Our Method        |
| t=0                 | A1:         |                                    | A1:          | A2:               |
| t=1                 | A1: Jupiter |                                    | A1: Jupiter  | A2: A             |
| t=2                 | A1: Jupiter | A2:                                | A1: Jupiter  | A3: very          |
| t=3                 | A1: Jupiter | A2: A                              | A1: Jupiter  | A3: very hot      |
| t=4                 | A1: Jupiter | A2: A small                        | A1: Jupiter  | A2: A small rocky |
| t=5                 | A1: Jupiter | A2: A small rocky                  |              | A3: very hot      |
| t=6                 | A1: Jupiter | A2: A small rocky core             |              |                   |
| t=7                 | A1: Jupiter | A2: A small rocky core             | A3: very     |                   |
| t=8                 | A1: Jupiter | A2: A small rocky core             | A3: very     |                   |
| t=9                 | A1: Jupiter | A2: A small rocky core             | A3: very hot |                   |

070

071 Figure 1: Overview of our method. The input is a prompt with a shared context and multiple questions.  
 072 Batch prompting (Cheng et al., 2023; Lin et al., 2024) concatenates all questions together, and the  
 073 output is generated sequentially using the typical LLM decoding method, taking 9 generation timesteps.  
 074 Our method generates the output in parallel and produces the result faster, taking only 3 generation  
 075 timesteps.

076

077

078 Our approach is a free lunch for batch prompting: it boosts throughput and memory efficiency without  
 079 requiring any model retraining and without compromising accuracy. The gains are largest when prefix  
 080 overlap is high and outputs are short to moderate, with the relative advantage tapering off as unique  
 081 suffixes grow longer. Unlike simple batch-prompting heuristics—which often degrade generation  
 082 quality by forcing the model to disentangle multiple requests within a single prompt—our method  
 083 avoids cross-query interference, supports flexible sharing groups, and fully exploits parallelism  
 084 throughout decoding.

085

## 086 2 BACKGROUND: ATTENTION MECHANISM

087

088 A core component of the Transformer is the attention computation. Given the sequence of queries  
 089  $Q \in \mathbb{R}^{N_q \times d}$ , keys  $K \in \mathbb{R}^{N_{kv} \times d}$ , values  $V \in \mathbb{R}^{N_{kv} \times d}$ , the transformer model computes the attention  
 090 output  $O \in \mathbb{R}^{N_q \times d}$  with the causal masking  $M$  as follows:

091

$$092 O = \text{Attention}(Q, K, V) = \text{softmax} \left( \frac{QK^T}{\sqrt{d}} + M \right) V \quad (1)$$

093

094 At the start of the generation process, a prefill stage processes the initial sequence of tokens that  
 095 the LLM will complete. During this stage, the entire prompt is encoded in parallel using a single  
 096 transformer forward pass. This results in a high number of queries and key-value pairs ( $N_q = N_{kv} \gg$   
 097 1), making the matrix multiplications in Equation 1 more hardware-friendly.

098

099 As the generation continues, completion tokens are decoded sequentially, with each decoding step  
 100 producing a new token and requiring a forward pass. To speed up this process, a KV cache is used  
 101 to store the attention keys and values of all previous tokens, eliminating the need to reprocess the  
 102

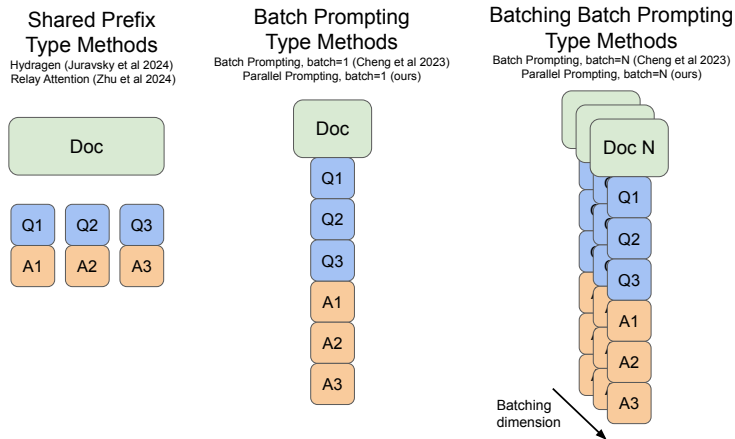
108 entire sequence during each decoding step. Instead, only the most recent token is passed through  
 109 the model. However, this approach results in a different attention computation where the number of  
 110 queries is 1 while the number of key-value pairs is still high ( $N_q = 1$  and  $N_{kv} \gg 1$ ). This leads to  
 111 matrix-vector products for the multiplications with  $K^T$  and  $V$ , making the attention during decoding  
 112 memory-bound and not utilizing tensor cores.  
 113

### 114 3 METHOD

#### 116 3.1 PROBLEM SETUP AND MOTIVATION

118 Consider a scenario where we have a shared context  $Doc$  (e.g., a document) and  $n$  questions  $q_1, \dots, q_n$   
 119 to answer based on this context. We want to generate answers  $A = \{a_1, a_2, \dots, a_n\}$  efficiently.

120 **Standard Approach with Shared Prefix.** The baseline processes each query independently, computing  
 121 each answer as  $a_i = \pi_{LLM}(Doc, q_i)$ , where  $\pi_{LLM}$  denotes the language model. For every query,  
 122 the model performs a *prefill* pass or reuses part of the cache over the concatenated input  $(Doc, q_i)$   
 123 and then executes a sequence of *incremental decode* steps to autoregressively generate the tokens of  
 124  $a_i$ . Answering  $n$  queries requires repeating the computationally expensive generation stage  $n$  times,  
 125 which dominates overall runtime.  
 126



142 Figure 2: Methods for efficiently handling multiple prompts with a shared prefix. **Shared prefix type**  
 143 **methods**, such as Hydragen and Relay Attention, batch together multiple questions and process them  
 144 in parallel. **Batch prompting type methods** put multiple prompts together into one prompt, which  
 145 can batch multiple documents together (**Batching Batch Prompting**).  
 146

147 **Batch Prompting Type Methods(SeqBatch)** (Cheng et al., 2023; Lin et al., 2024). A straightforward  
 148 attempt to avoid redundant computation is to concatenate all queries into a single prompt and let the  
 149 model generate a single long sequence containing all answers (see Figure 2, middle). While this  
 150 approach amortizes the cost of encoding the shared context  $Doc$ , it introduces a *prompt interference*  
 151 problem: due to the autoregressive nature of decoding, the model’s hidden state at step  $i$  contains all  
 152 previously generated tokens. Consequently, the answer for query  $i$  becomes implicitly conditioned  
 153 on other questions and earlier answers, and the resulting outputs are no longer independent. This  
 154 entanglement often degrades answer quality.  
 155

156 **Our Approach (Parallel Prompting).** We propose a method that generates all  $n$  answers in parallel  
 157 while ensuring that each answer remains conditioned only on its own query and the shared context.  
 158 The central idea is to apply query-specific attention masks during both the prefill and decoding stages  
 159 (see Figure 2, right), thereby isolating each question–answer flow while still enabling extensive  
 160 sharing of computation. This yields three key advantages:  
 161

1. *Shared-context prefill*: the computationally intensive encoding of  $Doc$  is executed once and  
 reused for all queries;

162        2. *Parallel decoding*: at every generation step, the model produces multiple next tokens  
 163        simultaneously for each query in a single batched forward pass;  
 164  
 165        3. *Independence of answers*: attention masking prevents cross-query information leakage,  
 166        ensuring that the generation of  $a_i$  depends solely on  $(Doc, q_i)$ .

167  
 168        Together, these mechanisms substantially reduce computation while preserving the independence and  
 169        quality of the generated answers.

170        Our method integrates seamlessly with the batching technique. By batching texts with multiple unique  
 171        documents and corresponding questions, efficiency can be improved further. Parallel generation  
 172        with batching provides two distinct advantages: firstly, inference throughput is further amplified by  
 173        batching with multiple unique prefix documents; secondly, it enables the balancing of batch size and  
 174        sequence length for model input, optimizing overall performance.

### 175        3.2 PARALLEL GENERATION WITH PROMPT-WISE INDEPENDENT ENCODING

176        Our method operates in two stages: **Prefill** and **Parallel Decode**.

177  
 178        **Prefill Stage.** We concatenate all queries into a single input sequence and encode them jointly together  
 179        with the shared context). To avoid any form of cross-query interference, we construct a query-specific  
 180        attention mask (see Figure 1, right) that ensures each query token attends only to the shared context  
 181        and to its own query tokens. This masking scheme is related to prepacking (Zhao et al., 2024), but  
 182        here we extend it to support multiple independent decoding streams simultaneously. To preserve  
 183        positional consistency, tokens for each query are assigned disjoint position indices immediately  
 184        following the shared-context sequence. If the shared context has been previously prefetched, we  
 185        directly reuse its KV-cache, thereby avoiding redundant prefill computation.

186  
 187        **Parallel Decoding Stage.** During autoregressive generation, we replace the standard one-token-per-  
 188        query decoding pattern with a fully *parallel* decoding scheme. The SeqBatch method processes all  
 189        documents and questions sequentially within a single batch. In contrast, the parallel generation method  
 190        employs efficient matrix operations to process multiple documents and questions simultaneously,  
 191        significantly accelerating the generation process by leveraging parallel computation capabilities.  
 192        In each forward pass, the model generates  $n$  tokens simultaneously (see Figure 1, right). This  
 193        transforms attention operations from a sequence of memory-bound matrix–vector products into a  
 194        single compute-bound matrix–matrix multiplication, resulting in significantly higher GPU utilization.  
 195        The attention masks defined during prefill are reused at every decoding step and expanded following  
 196        the same structural pattern, guaranteeing strict separation of decoding streams throughout generation.

197        The full algorithmic description is provided in Algorithm 1.

198  
 199        Since all questions are independent conditioned on the shared context, their answer distributions can  
 200        be computed simultaneously. To support this, we allow the model to generate  $N$  next-token logits in  
 201        a single forward pass, which corresponds to constructing a query matrix  $Q$  of shape  $N \times d$  in the  
 202        attention module.

203        During decoding, our method generates tokens for all questions in parallel. In each forward step, the  
 204        model extends the sequence with  $N$  new tokens—one per question. To maintain positional correctness,  
 205        we track the final prefix position of each stream and increment the corresponding positional index  
 206        before appending new tokens. After each step, the newly generated tokens are inserted into their  
 207        respective query streams, and the attention masks are updated according to the fixed pattern defined  
 208        during prefill. Because the mask structure is predetermined, only lightweight incremental updates are  
 209        required.

### 210        3.3 THEORETICAL ANALYSIS

211  
 212        In this section, we present a theoretical analysis of the parallel prompting method, focusing on  
 213        its efficiency gains in LLM inference. We begin by discussing the implications of Amdahl’s Law  
 214        in the context of parallel algorithms, followed by an examination of the speedup and throughput  
 215        improvements achieved through our approach.

---

216 **Algorithm 1** Parallel\_Batch\_Prompting: Parallel Prompt Generation with Shared-Prefix Cache

217 **Require:** Shared prefix Doc, unique suffix set  $Q_{\text{all}}$ , batch size  $N$ , parallel size  $P$ , language model

218  $\pi_{\text{LLM}}$

219 **Ensure:** List of generated answers

220 1: Optional:  $\text{cache} \leftarrow \text{PRECOMPUTE}(\pi_{\text{LLM}}, \text{Doc})$  ▷ Prefill KV-cache for shared prefix

221 2:  $i \leftarrow 0$

222 3:  $N_p \leftarrow N / P$  ▷ Samples per parallel group

223 4: **while**  $i < |Q_{\text{all}}|$  **do**

224 5:    $Q_n \leftarrow Q_{\text{all}}[i : i + N]$

225 6:    $Q_{np} \leftarrow \text{PARALLELIZEINTERLEAVE}(Q_n, P)$

226 7:    $\text{prompts} \leftarrow \text{PREPAREINPUT}(\text{Doc}, Q_{np}, N_p)$

227 8:    $\text{masks} \leftarrow \text{PREPAREMASK}(\text{prompts})$

228 9:    $\text{answers}, \text{output\_mask} \leftarrow \text{PARALLELGENERATE}(\pi_{\text{LLM}}, \text{prompts}, \text{masks}, P, \text{cache})$

229 10: **for**  $n = 1$  **to**  $N_p$  **do**

230 11:   **for**  $p = 1$  **to**  $P$  **do**

231 12:      $\text{final\_answer.append}(\text{DECODE}(\text{answers}[n, p], \text{output\_mask}[n, p]))$

232 13:   **end for**

233 14: **end for**

234 15:    $i \leftarrow i + N$

235 16: **end while**

236 17: **return**  $\text{final\_answer}$

237 18:

238 19: **function**  $\text{PARALLELGENERATE}(\pi_{\text{LLM}}, \text{prompts}, \text{masks}, P, \text{cache})$

239 20:    $\text{finished} \leftarrow \text{False}$

240 21:    $\text{input\_ids} \leftarrow \text{TOKENIZE}(\text{prompts})$

241 22:   **while** **not**  $\text{finished}$  **do**

242 23:      $\text{outputs} \leftarrow \pi_{\text{LLM}}.\text{FORWARD}(\text{input\_ids}, \text{masks}, \text{cache})$

243 24:      $\text{logits} \leftarrow \text{outputs}[:, -P:]$  ▷ Outputs  $P$  logits on sequence dimension

244 25:      $\text{next\_tokens} \leftarrow \text{SAMPLE}(\text{logits})$

245 26:      $\text{input\_ids} \leftarrow \text{CONCAT}(\text{input\_ids}, \text{next\_tokens})$

246 27:     **if**  $\text{STOPPINGCRITERIA}(\text{input\_ids})$  **then**

247 28:        $\text{finished} \leftarrow \text{True}$

248 29:     **else**

250 30:        $\text{masks} \leftarrow \text{UPDATEPARALLELMASK}(\text{input\_ids}, P)$

251 31:     **end if**

252 32:   **end while**

253 33:   **return**  $\text{input\_ids}, \text{masks}$

254 34: **end function**

255 35:

256 36: **function**  $\text{PRECOMPUTE}(\pi_{\text{LLM}}, \text{Doc})$

257 37:    $\text{kv\_cache} \leftarrow \pi_{\text{LLM}}.\text{FORWARD}(\text{Doc})$

258 38:   **return**  $\text{kv\_cache}$

259 39: **end function**

---

258 Amdahl’s Law provides a theoretical framework for understanding the potential speedup of a task  
259 when a portion of it is parallelized. It is defined as:

260

$$S(N) = \frac{1}{(1-p) + \frac{p}{N}} \quad (2)$$

261 where  $S(N)$  is the speedup with  $N$  processors,  $p$  is the fraction of the task that can be parallelized,  
262  $1-p$  is the fraction that remains serial. This law highlights that the overall speedup is limited by  
263 the serial portion of the task. As  $N$  increases, the speedup approaches  $\frac{1}{1-p}$ , indicating diminishing  
264 returns if  $p$  is not close to 1.

265 In the context of LLM inference, traditional methods process each query sequentially, leading to  
266 inefficiencies due to the serial nature of prompt processing. Our proposed method introduces parallel  
267 prompting, allowing multiple queries to be processed simultaneously. This approach effectively

270 maximizes throughput and reduces the time of the LLM’s inference task. We measure throughput as  
 271 queries (prompts) processed (a full output completion is generated) per unit time.

272 **Theorem 1** (Amdahl’s Law for Inference Throughput Improvement). *The throughput improvement  
 273  $\Delta$  (tasks processed per unit time above baseline) from using  $N$ -way parallel inference is:*

$$275 \quad \Delta = \frac{N \cdot S(N) - 1}{T_{\text{seq}}} \quad (3)$$

276 *See proofs and further details in Equation A.1.*

277 **Proposition 2.** *Consider inference on  $N$  independent queries using (a) standard batch processing  
 278 and (b) parallel prompting (packing all queries as independent subsequences in a single sequence  
 279 with attention masking).*

280 *Let  $T_{\text{batch}} = T_{\text{setup}} + N \cdot T_{\text{MV}}$  be the wall-time for a batch (with matrix-vector attention), and  
 281  $T_{\text{parallel}} = T_{\text{setup}} + T_{\text{MM}}$  for parallel prompting (with matrix-matrix attention). Then, the respective  
 282 throughput values are:*

$$283 \quad \text{Throughput}_{\text{batch}} = \frac{N}{T_{\text{batch}}}, \quad \text{Throughput}_{\text{parallel}} = \frac{N}{T_{\text{parallel}}} \quad (4)$$

284 *and*

$$285 \quad \frac{\text{Throughput}_{\text{parallel}}}{\text{Throughput}_{\text{batch}}} = \frac{T_{\text{batch}}}{T_{\text{parallel}}} = \frac{T_{\text{setup}} + NT_{\text{MV}}}{T_{\text{setup}} + T_{\text{MM}}} \quad (5)$$

286 *where  $T_{\text{MV}}$  is per-query wall-time for the matrix-vector attentions, and  $T_{\text{MM}}$  is wall-time for the  
 287 matrix-matrix product in the attention.*

288 *In practical settings, due to the efficiency of matrix multiplications on a GPU,  $T_{\text{MM}} \approx T_{\text{MV}}$ . If  
 289  $T_{\text{setup}} \ll T_{\text{MM}}$ , then  $\text{Throughput}_{\text{parallel}}$  is up to  $N \times$  that of standard batching.*

290 While the theoretical analysis suggests significant improvements, practical factors such as com-  
 291 munication overhead, memory bandwidth constraints, and synchronization costs can impact actual  
 292 performance. It is essential to consider these factors when implementing parallel prompting to ensure  
 293 that the theoretical gains translate into real-world efficiency.

### 302 3.4 THROUGHPUT MAXIMIZATION BY BALANCING ATTENTION PARALLELISM AND BATCH 303 SIZE

304 The use of batching is a crucial technique to enhance throughput in LLM inference. Through  
 305 batched decoding, each forward pass of the model processes the latest token from multiple sequences  
 306 concurrently rather than just one. This approach amplifies the arithmetic intensity of transformer  
 307 components, such as the multilayer perceptron (MLP) blocks, and facilitates the use of hardware-  
 308 friendly matrix multiplications.

309 However, the computation intensity of attention does not inherently benefit from batching, as each  
 310 sequence possesses its distinct key and value matrix. Consequently, while other model components  
 311 can leverage tensor cores during batched decoding, attention is required to be computed using  
 312 numerous independent matrix-vector products. Our parallel generation technique aims to address this  
 313 by enhancing the computation intensity of attention.

314 **Proposition 3** (Throughput Maximization). *Let  $P$  be the parallel size (number of independent queries  
 315 packed into a sequence for matrix-matrix attention),  $B$  the batch size (number of such sequences  
 316 processed in parallel), and  $P \cdot B \leq S^*$  a hardware resource constraint (e.g., total token capacity).*

317 *Let  $T_{\text{attn}}(P)$  denote the attention computation cost (function of  $P$ ), and  $T_{\text{mlp}}(B)$  denote the  
 318 MLP/other backend (function of  $B$ ).*

319 *Then, the throughput (queries per unit time) satisfies:*

$$320 \quad \text{Throughput}(P, B) = \frac{P \cdot B}{T_{\text{attn}}(P) + T_{\text{mlp}}(B)} \quad (6)$$

324 and maximal throughput is achieved at  
 325

$$(P^*, B^*) = \arg \max_{P \cdot B \leq S^*} \frac{P \cdot B}{T_{\text{attn}}(P) + T_{\text{mlp}}(B)} \quad (7)$$

328 where  $T_{\text{attn}}(P)$  generally improves with  $P$  up to a hardware limit (then degrades), and  $T_{\text{mlp}}(B)$   
 329 improves with  $B$  up to a limit.  
 330

331 The maximizing pair  $(P^*, B^*)$  is found by balancing optimal matrix-matrix utilization for attention  
 332 and optimal batch size for MLP efficiency. The throughput function is quasi-concave in  $(P, B)$  under  
 333 natural hardware scaling assumptions for transformer kernels. The theoretical maximum exists at an  
 334 interior point determined by hardware and model specifics, and is not achieved by maximizing either  
 335  $P$  or  $B$  alone.  
 336

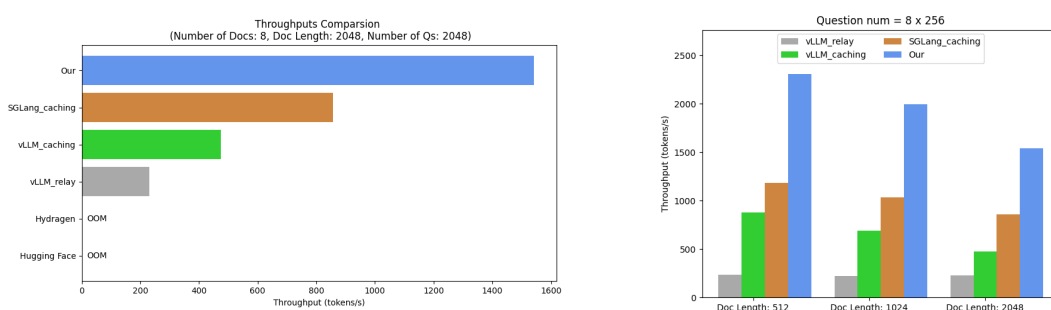
## 337 4 EXPERIMENTS

339 We evaluate our method through two complementary sets of experiments: (1) controlled scaling  
 340 studies on small and medium-sized models using synthetic data, and (2) a downstream task evaluation  
 341 on reading comprehension datasets using Llama 3-8B. This combination enables both fine-grained  
 342 analysis of computational behavior and validation on a realistic application. All experiments are  
 343 conducted on a single NVIDIA A100-80GB GPU using PyTorch implementations built on the  
 344 HuggingFace architecture (Wolf et al., 2020). Additional implementation details are provided in  
 345 Appendix B.  
 346

### 347 4.1 SCALING EXPERIMENTS

348 **Setup.** Following Juravsky et al. (2024), we construct synthetic datasets with varying document  
 349 lengths, numbers of unique documents, and numbers of queries. Document content is drawn from a  
 350 subset of *War and Peace* (Tolstoy, 1869), with procedurally generated sentences added for greater  
 351 length diversity. We perform all scaling studies on CodeLlama-7B-Instruct (Rozière et al., 2024),  
 352 Sheared-LLaMA-1.3B (Xia et al., 2024), and LLaMA-160M (Miao et al., 2023) to enable controlled  
 353 analysis under constrained compute.  
 354

355 **Memory Constraints and Throughput Under Increasing Context Length.** We first examine  
 356 memory usage and throughput as the number of queries and the shared-context length increase. Figure  
 357 3 summarizes the results. Several baselines (e.g., HuggingFace with DynamicCache, Hydragen)  
 358 encounter out-of-memory failures at high query counts, whereas our method remains stable. As  
 359 shown in the right panel of Figure 3, throughput decreases with longer prefixes for all methods, but  
 360 our parallel prompting consistently achieves higher throughput without sacrificing generation quality.  
 361 A full breakdown of memory measurements across all conditions appears in Table 6 and Table 5 in  
 362 the Appendix.  
 363



374 Figure 3: **Left:** Memory usage for multiple prefix-sharing methods under increasing numbers  
 375 of queries with CodeLlama-7B-Instruct on an A100 GPU. **Right:** Throughput comparison for  
 376 CodeLlama-7B-Instruct on an A100 GPU as the shared-context length increases. We fix 256 total  
 377 queries, 8 unique documents, a query length of 12, and generate 5 tokens per query.  
 378

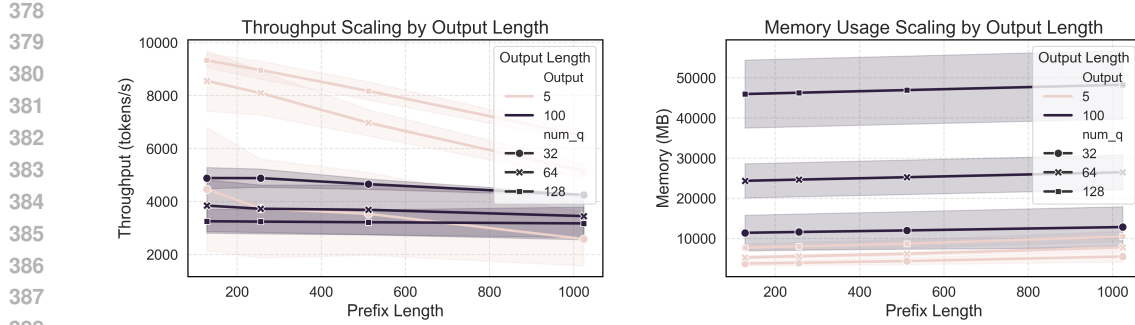


Figure 4: **Left:** Throughput (tokens/sec) as a function of prefix and output lengths with CodeLlama-7B-Instruct on an A100 GPU; lines correspond to different output lengths, markers denote the number of queries. **Right:** GPU memory usage with varying prefix and output lengths. Results shown for 4 documents and 32 queries.

**Scaling with Output Length.** To further isolate computational factors, we study performance as a function of generated output length. Figure 4 reports both throughput and GPU memory usage across varying prefix and output lengths. Longer prefixes and outputs impose higher computational load, but our method maintains efficiency and stable scaling.

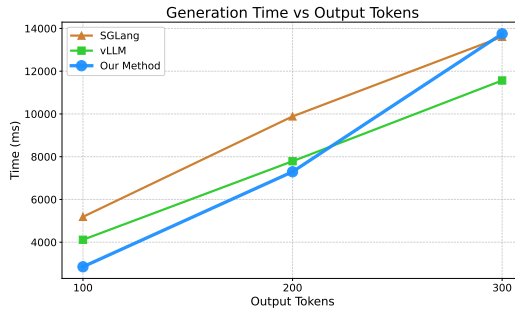


Figure 5: Comparison of generation time versus output tokens for our method, vLLM and SGLang with CodeLlama-7B-Instruct on an A100 GPU. As the number of output tokens increases, both methods require more time; however, our method consistently achieves lower generation time for shorter outputs and remains competitive as the output length grows. The blue line represents our method, while the light green line represents vLLM and the orange line represents SGLang, both evaluated with 4 documents and 32 questions per batch.

We also conduct experiments varying output length up to 300 tokens. Results on our syntactic dataset in Figure 5 show that Parallel Prompting consistently delivers throughput gains over the vLLM method up to approximately 200 output tokens per question. As an example, for four unique documents with  $4 \times 32$  questions, our method required 7,295 milliseconds (throughput  $\approx 3,500$  tokens/sec), while the vLLM method takes 7,605 milliseconds (throughput  $\approx 3,360$  tokens/sec). When the output length exceeds 200 tokens, vLLM may offer a greater advantage.

**Batch Size vs. Parallel Size.** We next analyze how throughput depends jointly on batch size and parallel size. Intuitively, increasing parallel size improves efficiency up to a point, after which larger batch sizes provide better arithmetic intensity. Figure 6 (left and middle) illustrates that the optimal throughput is achieved by balancing these two factors. Our preliminary results suggest that longer prefixes prefer larger parallel size, as also visible in Figure 6 (Left). A detailed numerical comparison for 1B and 7B models appears in Table 4 in the Appendix. However, due to limited resources, we were unable to perform a comprehensive sweep across many model sizes and hardware settings.

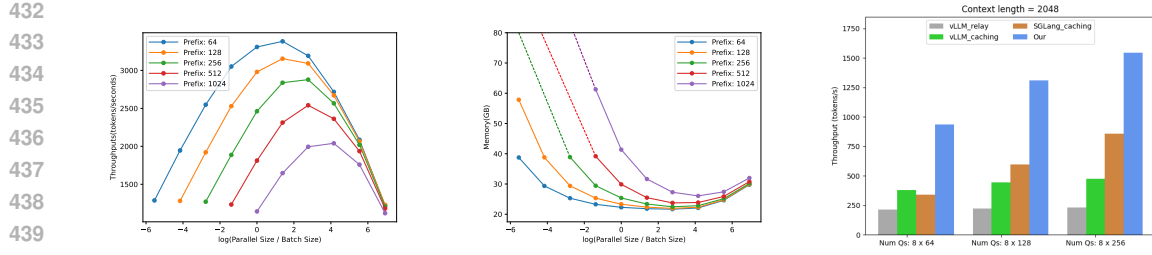


Figure 6: **Left:** Throughput comparison for 1024 queries across multiple document settings with CodeLlama-7B-Instruct on an A100 GPU. The X-axis represents the logarithm of the ratio between the parallel size and the batch size. This metric is used to show that these two parameters must be balanced to achieve maximum inference throughput. **Middle:** GPU memory usage for the same settings. **Right:** Throughput under long-context inference. Notation such as  $8 \times 64$  means there are 8 unique documents, and each document has 64 associated questions (total = 512 questions).

## 4.2 CASE STUDY: QUESTION ANSWERING PERFORMANCE

We evaluate our method on downstream reading comprehension tasks to assess end-to-end impact on both quality and generation speed. We use Llama 3-8B (Grattafiori et al., 2024) and measure F1 scores (standard for QA) on SQuAD (Rajpurkar et al., 2016), QuAC (Choi et al., 2018), and DROP (Dua et al., 2019).

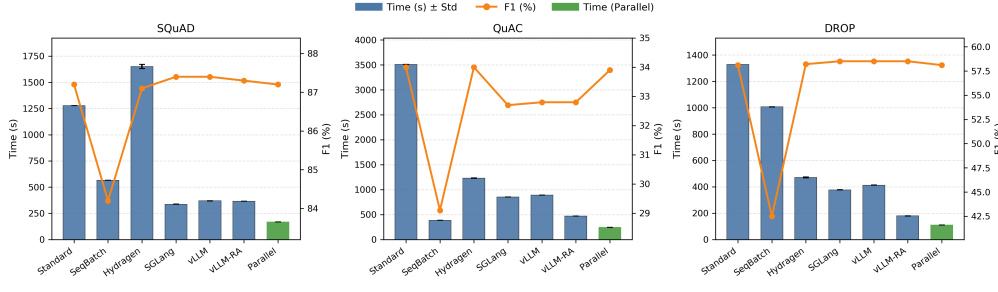


Figure 7: Comparison of generation time and F1 performance across prompting methods using Llama 3-8B on an A100 GPU. Reported results are averaged over five runs.

As shown in Figure 7, our parallel prompting achieves substantially lower latency compared to standard prompting, sequential batching, Hydragen, SGLang, vLLM (with and without relay attention), while maintaining equivalent answer quality across all datasets.

## 5 RELATED WORK

Recent advancements in language modeling have delved into the prediction of multiple tokens simultaneously to enhance both efficiency and performance. Notable works such as (Miao et al., 2024; Leviathan et al., 2023; Wu et al., 2024) focus on speculative decoding methods, where potential future sequences are built and verified to expedite inference. Similarly, (Gloeckle et al., 2024) and (Cai et al., 2024) propose predicting multiple future tokens using different output heads, thereby speeding up the inference process. Efforts to increase throughput in LLM inference have led to various innovative techniques aimed at optimizing GPU utilization and improving throughput. (Dao et al., 2022) and (Sheng et al., 2023) aim to improve memory usage efficiency, enabling higher throughput in generative inference tasks. (Jin et al., 2023) schedules prompts based on estimated output sequence lengths to optimize GPU usage. (Gim et al., 2024) proposes reusing precomputed caches in a predefined schema to reduce latency. (Sun et al., 2024) applies dynamic sparse KV caching in decoding to accelerate long sequence generation. Efficient prompting techniques could also increase the throughput of LLM. (Cheng et al., 2023) groups multiple questions in a single prompt,

486 though it will lead to performance degradation when the number of questions increases. (Zhao et al.,  
 487 2024) enhances throughput during the prefilling stage by prepacking data. (Ning et al., 2024) uses  
 488 the skeleton of the answer to batch-generate the final answer. To avoid the KV cache duplication,  
 489 existing work (Kwon et al., 2023) vLLM uses its PagedAttention and paged memory management  
 490 to point multiple identical input prompts to only one physical block across multiple queries. Also,  
 491 (Juravsky et al., 2024) proposes a decomposition of attention computation of shared prefixes and  
 492 unique suffixes. (Lu et al., 2024) increases efficiency by sharing cache in the encoder-decoder model  
 493 for decomposable tasks. Compared with the above methods, our work introduces a novel inference  
 494 technique that allows LLMs to leverage GPU parallel capacity to improve inference throughput and  
 495 memory utilization without degrading reasoning performance.

## 496 6 CONCLUSION

497 We introduce an efficient parallel prompting method for decoding prompt queries in parallel. We  
 498 conduct experiments with multiple downstream datasets, constructed synthetic data, and show our  
 499 method achieves improvements in throughput and computational resource management, offering a  
 500 robust solution for different tasks in LLMs.

## 501 LIMITATIONS

502 **Skewed Generation Lengths** Our method achieves the highest throughput gains when suffix  
 503 lengths are similar, and performance may degrade when generation lengths are highly skewed during  
 504 decoding. To mitigate this, we propose several practical strategies: In cases where generation lengths  
 505 become highly unbalanced, the system can fall back to standard inference. In real-world applications,  
 506 expected output length can often be heuristically estimated based on properties such as question and  
 507 context length. This enables grouping questions with similar expected output lengths, minimizing  
 508 skew. More advanced solutions, such as dynamic batching (e.g., as introduced in Verl), could be  
 509 adopted to support streaming scenarios and further optimize batching efficiency.

510 **Prompt-Agnostic Batching** Our method’s gains are largest when there is a clear shared-prefix  
 511 structure and output lengths are short to moderate. As the length of unique suffixes increases, the  
 512 benefit of parallel generation diminishes, since more computation must be performed individually for  
 513 each query. For very long outputs, prompt-agnostic batching (such as vLLM’s default scheduling)  
 514 may outperform our approach. We recommend a hybrid scheduling policy in production, using  
 515 Parallel Prompting for workloads with substantial shared context and prompt-agnostic batching for  
 516 others. This method is designed to complement, not replace, existing batching strategies.

## 517 REPRODUCIBILITY STATEMENT

518 We have taken several steps to facilitate reproducibility. Assumptions and proofs for all theoretical  
 519 claims are provided in Appendix [A], which states all conditions under which the results hold.  
 520 Experimental settings—including datasets, preprocessing, model configurations, training schedules,  
 521 hyperparameters, and evaluation protocols in Section Experiments. An anonymized, self-contained  
 522 supplementary .zip archive includes source code and scripts to reproduce the main tables/figures and  
 523 ablations. Known limitations, potential failure modes, and scope of applicability are discussed in  
 524 Section Limitations. Any deviations from the default procedures or additional implementation notes  
 525 are included in Appendix [B].

## 526 REFERENCES

527 Tianle Cai, Yuhong Li, Zhengyang Geng, Hongwu Peng, Jason D Lee, Deming Chen, and Tri Dao.  
 528 Medusa: Simple llm inference acceleration framework with multiple decoding heads. *arXiv  
 529 preprint arXiv:2401.10774*, 2024.

530 Zhoujun Cheng, Jungo Kasai, and Tao Yu. Batch prompting: Efficient inference with large language  
 531 model apis. *arXiv preprint arXiv:2301.08721*, 2023.

540 Eunsol Choi, He He, Mohit Iyyer, Mark Yatskar, Wen-tau Yih, Yejin Choi, Percy Liang, and Luke  
 541 Zettlemoyer. Quac: Question answering in context. *arXiv preprint arXiv:1808.07036*, 2018.  
 542

543 Tri Dao, Dan Fu, Stefano Ermon, Atri Rudra, and Christopher Ré. Flashattention: Fast and memory-  
 544 efficient exact attention with io-awareness. *Advances in Neural Information Processing Systems*,  
 545 35:16344–16359, 2022.

546 Dheeru Dua, Yizhong Wang, Pradeep Dasigi, Gabriel Stanovsky, Sameer Singh, and Matt Gardner.  
 547 Drop: A reading comprehension benchmark requiring discrete reasoning over paragraphs. *arXiv  
 548 preprint arXiv:1903.00161*, 2019.  
 549

550 In Gim, Guojun Chen, Seung-seob Lee, Nikhil Sarda, Anurag Khandelwal, and Lin Zhong. Prompt  
 551 cache: Modular attention reuse for low-latency inference. *Proceedings of Machine Learning and  
 552 Systems*, 6:325–338, 2024.

553 Fabian Gloeckle, Badr Youbi Idrissi, Baptiste Rozière, David Lopez-Paz, and Gabriel Synnaeve.  
 554 Better & faster large language models via multi-token prediction. *arXiv preprint arXiv:2404.19737*,  
 555 2024.  
 556

557 Aaron Grattafiori, Abhimanyu Dubey, Abhinav Jauhri, Abhinav Pandey, Abhishek Kadian, Ahmad  
 558 Al-Dahle, Aiesha Letman, Akhil Mathur, Alan Schelten, Alex Vaughan, Amy Yang, Angela Fan,  
 559 Anirudh Goyal, Anthony Hartshorn, Aobo Yang, Archi Mitra, Archie Sravankumar, Artem Korenev,  
 560 Arthur Hinsvark, Arun Rao, Aston Zhang, Aurelien Rodriguez, Austen Gregerson, Ava Spataru,  
 561 Baptiste Roziere, Bethany Biron, Binh Tang, Bobbie Chern, Charlotte Caucheteux, Chaya Nayak,  
 562 Chloe Bi, Chris Marra, Chris McConnell, Christian Keller, Christophe Touret, Chunyang Wu,  
 563 Corinne Wong, Cristian Canton Ferrer, Cyrus Nikolaidis, Damien Allonsius, Daniel Song, Danielle  
 564 Pintz, Danny Livshits, Danny Wyatt, David Esiobu, Dhruv Choudhary, Dhruv Mahajan, Diego  
 565 Garcia-Olano, Diego Perino, Dieuwke Hupkes, Egor Lakomkin, Ehab AlBadawy, Elina Lobanova,  
 566 Emily Dinan, Eric Michael Smith, Filip Radenovic, Francisco Guzmán, Frank Zhang, Gabriel  
 567 Synnaeve, Gabrielle Lee, Georgia Lewis Anderson, Govind Thattai, Graeme Nail, Gregoire Mialon,  
 568 Guan Pang, Guillem Cucurell, Hailey Nguyen, Hannah Korevaar, Hu Xu, Hugo Touvron, Iliyan  
 569 Zarov, Imanol Arrieta Ibarra, Isabel Kloumann, Ishan Misra, Ivan Evtimov, Jack Zhang, Jade Copet,  
 570 Jaewon Lee, Jan Geffert, Jana Vraneš, Jason Park, Jay Mahadeokar, Jeet Shah, Jelmer van der Linde,  
 571 Jennifer Billock, Jenny Hong, Janya Lee, Jeremy Fu, Jianfeng Chi, Jianyu Huang, Jiawen Liu, Jie  
 572 Wang, Jiecao Yu, Joanna Bitton, Joe Spisak, Jongsoo Park, Joseph Rocca, Joshua Johnstun, Joshua  
 573 Saxe, Junteng Jia, Kalyan Vasudevan Alwala, Karthik Prasad, Kartikeya Upasani, Kate Plawiak,  
 574 Ke Li, Kenneth Heafield, Kevin Stone, Khalid El-Arini, Krithika Iyer, Kshitiz Malik, Kuenley  
 575 Chiu, Kunal Bhalla, Kushal Lakhota, Lauren Rantala-Yeary, Laurens van der Maaten, Lawrence  
 576 Chen, Liang Tan, Liz Jenkins, Louis Martin, Lovish Madaan, Lubo Malo, Lukas Blecher, Lukas  
 577 Landzaat, Luke de Oliveira, Madeline Muzzi, Mahesh Pasupuleti, Mannat Singh, Manohar Paluri,  
 578 Marcin Kardas, Maria Tsimpoukelli, Mathew Oldham, Mathieu Rita, Maya Pavlova, Melanie  
 579 Kambadur, Mike Lewis, Min Si, Mitesh Kumar Singh, Mona Hassan, Naman Goyal, Narjes  
 580 Torabi, Nikolay Bashlykov, Nikolay Bogoychev, Niladri Chatterji, Ning Zhang, Olivier Duchenne,  
 581 Onur Çelebi, Patrick Alrassy, Pengchuan Zhang, Pengwei Li, Petar Vasic, Peter Weng, Prajwal  
 582 Bhargava, Pratik Dubal, Praveen Krishnan, Punit Singh Koura, Puxin Xu, Qing He, Qingxiao Dong,  
 583 Ragavan Srinivasan, Raj Ganapathy, Ramon Calderer, Ricardo Silveira Cabral, Robert Stojnic,  
 584 Roberta Raileanu, Rohan Maheswari, Rohit Girdhar, Rohit Patel, Romain Sauvestre, Ronnie  
 585 Polidoro, Roshan Sumbaly, Ross Taylor, Ruan Silva, Rui Hou, Rui Wang, Saghar Hosseini, Sahana  
 586 Chennabasappa, Sanjay Singh, Sean Bell, Seohyun Sonia Kim, Sergey Edunov, Shaoliang Nie,  
 587 Sharan Narang, Sharath Raparthi, Sheng Shen, Shengye Wan, Shruti Bhosale, Shun Zhang, Simon  
 588 Vandenhende, Soumya Batra, Spencer Whitman, Sten Sootla, Stephane Collot, Suchin Gururangan,  
 589 Sydney Borodinsky, Tamar Herman, Tara Fowler, Tarek Sheasha, Thomas Georgiou, Thomas  
 590 Scialom, Tobias Speckbacher, Todor Mihaylov, Tong Xiao, Ujjwal Karn, Vedanuj Goswami,  
 591 Vibhor Gupta, Vignesh Ramanathan, Viktor Kerkez, Vincent Gonguet, Virginie Do, Vish Vogeti,  
 592 Vitor Albiero, Vladan Petrovic, Weiwei Chu, Wenhan Xiong, Wenyin Fu, Whitney Meers, Xavier  
 593 Martinet, Xiaodong Wang, Xiaofang Wang, Xiaoqing Ellen Tan, Xide Xia, Xinfeng Xie, Xuchao  
 Jia, Xuewei Wang, Yaelle Goldschlag, Yashesh Gaur, Yasmine Babaei, Yi Wen, Yiwen Song,  
 Yuchen Zhang, Yue Li, Yuning Mao, Zacharie Delpierre Coudert, Zheng Yan, Zhengxing Chen, Zoe  
 Papakipos, Aaditya Singh, Aayushi Srivastava, Abha Jain, Adam Kelsey, Adam Shajnfeld, Adithya  
 Gangidi, Adolfo Victoria, Ahuva Goldstand, Ajay Menon, Ajay Sharma, Alex Boesenber, Alexei

594 Baevski, Allie Feinstein, Amanda Kallet, Amit Sangani, Amos Teo, Anam Yunus, Andrei Lupu,  
 595 Andres Alvarado, Andrew Caples, Andrew Gu, Andrew Ho, Andrew Poulton, Andrew Ryan, Ankit  
 596 Ramchandani, Annie Dong, Annie Franco, Anuj Goyal, Aparajita Saraf, Arkabandhu Chowdhury,  
 597 Ashley Gabriel, Ashwin Bharambe, Assaf Eisenman, Azadeh Yazdan, Beau James, Ben Maurer,  
 598 Benjamin Leonhardi, Bernie Huang, Beth Loyd, Beto De Paola, Bhargavi Paranjape, Bing Liu,  
 599 Bo Wu, Boyu Ni, Braden Hancock, Bram Wasti, Brandon Spence, Brani Stojkovic, Brian Gamido,  
 600 Britt Montalvo, Carl Parker, Carly Burton, Catalina Mejia, Ce Liu, Changhan Wang, Changkyu  
 601 Kim, Chao Zhou, Chester Hu, Ching-Hsiang Chu, Chris Cai, Chris Tindal, Christoph Feichtenhofer,  
 602 Cynthia Gao, Damon Civin, Dana Beaty, Daniel Kreymer, Daniel Li, David Adkins, David Xu,  
 603 Davide Testuggine, Delia David, Devi Parikh, Diana Liskovich, Didem Foss, Dingkang Wang, Duc  
 604 Le, Dustin Holland, Edward Dowling, Eissa Jamil, Elaine Montgomery, Eleonora Presani, Emily  
 605 Hahn, Emily Wood, Eric-Tuan Le, Erik Brinkman, Esteban Arcuate, Evan Dunbar, Evan Smothers,  
 606 Fei Sun, Felix Kreuk, Feng Tian, Filippos Kokkinos, Firat Ozgenel, Francesco Caggioni, Frank  
 607 Kanayet, Frank Seide, Gabriela Medina Florez, Gabriella Schwarz, Gada Badeer, Georgia Swee,  
 608 Gil Halpern, Grant Herman, Grigory Sizov, Guangyi, Zhang, Guna Lakshminarayanan, Hakan Inan,  
 609 Hamid Shojanazeri, Han Zou, Hannah Wang, Hanwen Zha, Haroun Habeeb, Harrison Rudolph,  
 610 Helen Suk, Henry Aspegen, Hunter Goldman, Hongyuan Zhan, Ibrahim Damlaj, Igor Molybog,  
 611 Igor Tufanov, Ilias Leontiadis, Irina-Elena Veliche, Itai Gat, Jake Weissman, James Geboski, James  
 612 Kohli, Janice Lam, Japhet Asher, Jean-Baptiste Gaya, Jeff Marcus, Jeff Tang, Jennifer Chan, Jenny  
 613 Zhen, Jeremy Reizenstein, Jeremy Teboul, Jessica Zhong, Jian Jin, Jingyi Yang, Joe Cummings,  
 614 Jon Carvill, Jon Shepard, Jonathan McPhie, Jonathan Torres, Josh Ginsburg, Junjie Wang, Kai  
 615 Wu, Kam Hou U, Karan Saxena, Kartikay Khandelwal, Katayoun Zand, Kathy Matosich, Kaushik  
 616 Veeraghavan, Kelly Michelena, Keqian Li, Kiran Jagadeesh, Kun Huang, Kunal Chawla, Kyle  
 617 Huang, Lailin Chen, Lakshya Garg, Lavender A, Leandro Silva, Lee Bell, Lei Zhang, Liangpeng  
 618 Guo, Licheng Yu, Liron Moshkovich, Luca Wehrstedt, Madian Khabsa, Manav Avalani, Manish  
 619 Bhatt, Martynas Mankus, Matan Hasson, Matthew Lennie, Matthias Reso, Maxim Groshev, Maxim  
 620 Naumov, Maya Lathi, Meghan Keneally, Miao Liu, Michael L. Seltzer, Michal Valko, Michelle  
 621 Restrepo, Mihi Patel, Mik Vyatskov, Mikayel Samvelyan, Mike Clark, Mike Macey, Mike Wang,  
 622 Miquel Jubert Hermoso, Mo Metanat, Mohammad Rastegari, Munish Bansal, Nandhini Santhanam,  
 623 Natascha Parks, Natasha White, Navyata Bawa, Nayan Singhal, Nick Egebo, Nicolas Usunier,  
 624 Nikhil Mehta, Nikolay Pavlovich Laptev, Ning Dong, Norman Cheng, Oleg Chernoguz, Olivia  
 625 Hart, Omkar Salpekar, Ozlem Kalinli, Parkin Kent, Parth Parekh, Paul Saab, Pavan Balaji, Pedro  
 626 Rittner, Philip Bontrager, Pierre Roux, Piotr Dollar, Polina Zvyagina, Prashant Ratanchandani,  
 627 Pritish Yuvraj, Qian Liang, Rachad Alao, Rachel Rodriguez, Rafi Ayub, Raghotham Murthy,  
 628 Raghu Nayani, Rahul Mitra, Rangaprabhu Parthasarathy, Raymond Li, Rebekkah Hogan, Robin  
 629 Battey, Rocky Wang, Russ Howes, Ruty Rinott, Sachin Mehta, Sachin Siby, Sai Jayesh Bondu,  
 630 Samyak Datta, Sara Chugh, Sara Hunt, Sargun Dhillon, Sasha Sidorov, Satadru Pan, Saurabh  
 631 Mahajan, Saurabh Verma, Seiji Yamamoto, Sharadh Ramaswamy, Shaun Lindsay, Shaun Lindsay,  
 632 Sheng Feng, Shenghao Lin, Shengxin Cindy Zha, Shishir Patil, Shiva Shankar, Shuqiang Zhang,  
 633 Shuqiang Zhang, Sinong Wang, Sneha Agarwal, Soji Sajuyigbe, Soumith Chintala, Stephanie  
 634 Max, Stephen Chen, Steve Kehoe, Steve Satterfield, Sudarshan Govindaprasad, Sumit Gupta,  
 635 Summer Deng, Sungmin Cho, Sunny Virk, Suraj Subramanian, Sy Choudhury, Sydney Goldman,  
 636 Tal Remez, Tamar Glaser, Tamara Best, Thilo Koehler, Thomas Robinson, Tianhe Li, Tianjun  
 637 Zhang, Tim Matthews, Timothy Chou, Tzook Shaked, Varun Vontimitta, Victoria Ajayi, Victoria  
 638 Montanez, Vijai Mohan, Vinay Satish Kumar, Vishal Mangla, Vlad Ionescu, Vlad Poenaru,  
 639 Vlad Tiberiu Mihaiescu, Vladimir Ivanov, Wei Li, Wenchen Wang, Wenwen Jiang, Wes Bouaziz,  
 640 Will Constable, Xiaocheng Tang, Xiaojian Wu, Xiaolan Wang, Xilun Wu, Xinbo Gao, Yaniv  
 641 Kleinman, Yanjun Chen, Ye Hu, Ye Jia, Ye Qi, Yenda Li, Yilin Zhang, Ying Zhang, Yossi Adi,  
 642 Youngjin Nam, Yu, Wang, Yu Zhao, Yuchen Hao, Yundi Qian, Yunlu Li, Yuzi He, Zach Rait,  
 643 Zachary DeVito, Zef Rosnbrick, Zhaoduo Wen, Zhenyu Yang, Zhiwei Zhao, and Zhiyu Ma. The  
 644 llama 3 herd of models, 2024. URL <https://arxiv.org/abs/2407.21783>.  
 645

646 Yunho Jin, Chun-Feng Wu, David Brooks, and Gu-Yeon Wei.  $s^3$ : Increasing gpu utilization during  
 647 generative inference for higher throughput. *Advances in Neural Information Processing Systems*,  
 648 36:18015–18027, 2023.

649 Jordan Juravsky, Bradley Brown, Ryan Ehrlich, Daniel Y Fu, Christopher Ré, and Azalia Mirhoseini.  
 650 Hydragren: High-throughput llm inference with shared prefixes. *arXiv preprint arXiv:2402.05099*,  
 651 2024.

648 Woosuk Kwon, Zhuohan Li, Siyuan Zhuang, Ying Sheng, Lianmin Zheng, Cody Hao Yu, Joseph  
 649 Gonzalez, Hao Zhang, and Ion Stoica. Efficient memory management for large language model  
 650 serving with pagedattention. In *Proceedings of the 29th Symposium on Operating Systems  
 651 Principles*, pp. 611–626, 2023.

652 Yaniv Leviathan, Matan Kalman, and Yossi Matias. Fast inference from transformers via speculative  
 653 decoding. In *International Conference on Machine Learning*, pp. 19274–19286. PMLR, 2023.

654 Jianzhe Lin, Maurice Diesendruck, Liang Du, and Robin Abraham. Batchprompt: Accomplish more  
 655 with less, 2024. URL <https://arxiv.org/abs/2309.00384>.

656 Bo-Ru Lu, Nikita Haduong, Chien-Yu Lin, Hao Cheng, Noah A Smith, and Mari Ostendorf. Encode  
 657 once and decode in parallel: Efficient transformer decoding. *arXiv preprint arXiv:2403.13112*,  
 660 2024.

661 Xupeng Miao, Gabriele Oliaro, Zhihao Zhang, Xinhao Cheng, Zeyu Wang, Rae Ying Yee Wong,  
 662 Zhuoming Chen, Daiyaan Arfeen, Reyna Abhyankar, and Zhihao Jia. Specinfer: Accelerating  
 663 generative llm serving with speculative inference and token tree verification, 2023.

664 Xupeng Miao, Gabriele Oliaro, Zhihao Zhang, Xinhao Cheng, Zeyu Wang, Zhengxin Zhang, Rae  
 665 Ying Yee Wong, Alan Zhu, Lijie Yang, Xiaoxiang Shi, et al. Specinfer: Accelerating large  
 666 language model serving with tree-based speculative inference and verification. In *Proceedings of  
 667 the 29th ACM International Conference on Architectural Support for Programming Languages  
 668 and Operating Systems, Volume 3*, pp. 932–949, 2024.

669 Xuefei Ning, Zinan Lin, Zixuan Zhou, Zifu Wang, Huazhong Yang, and Yu Wang. Skeleton-of-  
 670 thought: Prompting llms for efficient parallel generation. In *The Twelfth International Conference  
 671 on Learning Representations*, 2024.

672 Pranav Rajpurkar, Jian Zhang, Konstantin Lopyrev, and Percy Liang. Squad: 100,000+ questions for  
 673 machine comprehension of text, 2016. URL <https://arxiv.org/abs/1606.05250>.

674 Baptiste Rozière, Jonas Gehring, Fabian Gloeckle, Sten Sootla, Itai Gat, Xiaoqing Ellen Tan, Yossi  
 675 Adi, Jingyu Liu, Romain Sauvestre, Tal Remez, Jérémie Rapin, Artyom Kozhevnikov, Ivan Evtimov,  
 676 Joanna Bitton, Manish Bhatt, Cristian Canton Ferrer, Aaron Grattafiori, Wenhan Xiong, Alexandre  
 677 Défossez, Jade Copet, Faisal Azhar, Hugo Touvron, Louis Martin, Nicolas Usunier, Thomas  
 678 Scialom, and Gabriel Synnaeve. Code llama: Open foundation models for code, 2024. URL  
 679 <https://arxiv.org/abs/2308.12950>.

680 Ying Sheng, Lianmin Zheng, Binhang Yuan, Zhuohan Li, Max Ryabinin, Beidi Chen, Percy Liang,  
 681 Christopher Ré, Ion Stoica, and Ce Zhang. Flexgen: High-throughput generative inference of  
 682 large language models with a single gpu. In *International Conference on Machine Learning*, pp.  
 683 31094–31116. PMLR, 2023.

684 Hanshi Sun, Zhuoming Chen, Xinyu Yang, Yuandong Tian, and Beidi Chen. Triforce: Lossless  
 685 acceleration of long sequence generation with hierarchical speculative decoding. *arXiv preprint  
 686 arXiv:2404.11912*, 2024.

687 Leo Tolstoy. *War and Peace*. 1869.

688 Thomas Wolf, Lysandre Debut, Victor Sanh, Julien Chaumond, Clement Delangue, Anthony Moi,  
 689 Pierrick Cistac, Tim Rault, Rémi Louf, Morgan Funtowicz, et al. Transformers: State-of-the-art  
 690 natural language processing. In *Proceedings of the 2020 conference on empirical methods in  
 691 natural language processing: system demonstrations*, pp. 38–45, 2020.

692 Pengfei Wu, Jiahao Liu, Zhuocheng Gong, Qifan Wang, Jinpeng Li, Jingang Wang, Xunliang Cai, and  
 693 Dongyan Zhao. Parallel decoding via hidden transfer for lossless large language model acceleration.  
 694 *arXiv preprint arXiv:2404.12022*, 2024.

695 Mengzhou Xia, Tianyu Gao, Zhiyuan Zeng, and Danqi Chen. Sheared llama: Accelerating language  
 696 model pre-training via structured pruning, 2024. URL <https://arxiv.org/abs/2310.06694>.

702 Siyan Zhao, Daniel Israel, Guy Van den Broeck, and Aditya Grover. Prepacking: A simple method for  
703 fast prefilling and increased throughput in large language models. *arXiv preprint arXiv:2404.09529*,  
704 2024.

705 Lianmin Zheng, Liangsheng Yin, Zhiqiang Xie, Chuyue Sun, Jeff Huang, Cody Hao Yu, Shiyi Cao,  
706 Christos Kozyrakis, Ion Stoica, Joseph E Gonzalez, et al. Sglang: Efficient execution of structured  
707 language model programs. *arXiv preprint arXiv:2312.07104*, 2024.

709 Lei Zhu, Xinjiang Wang, Wayne Zhang, and Rynson WH Lau. Relayattention for efficient large  
710 language model serving with long system prompts. *arXiv preprint arXiv:2402.14808*, 2024.

711

712

713

714

715

716

717

718

719

720

721

722

723

724

725

726

727

728

729

730

731

732

733

734

735

736

737

738

739

740

741

742

743

744

745

746

747

748

749

750

751

752

753

754

755

756 A APPENDIX  
757758 A.1 PROOF OF THEOREM 1.  
759760 **Amdahl's Law for Inference Throughput Improvement** The throughput improvement  $\Delta$  (tasks  
761 processed per unit time above baseline) from using  $N$ -way parallel inference is:  
762

763 
$$\Delta = \frac{N \cdot S(N) - 1}{T_{\text{seq}}} \quad (8)$$
  
764

765 **Assumptions:**  
766767 

- Each inference computation can be split into a parallelizable fraction and a sequential  
768 fraction.
- There are  $N$  independent queries, each requiring  $T_{\text{seq}}$  execution time if performed sequentially.  
770
- There is no communication, scheduling, or parallelization overhead. Negligible coordination  
772 or resource contention.
- $N$  processors are available, and the parallel workload is divided equally among them. In  
774 parallel, independent  $N$  queries are processed in time  $T_{\text{par}}(N) = T_{\text{seq}}/S(N)$ , where  $S(N)$   
775 is given by Amdahl's law Equation 2

  
776777 *Proof of Theorem 1.* The sequential throughput is  $\frac{1}{T_{\text{seq}}}$ . With parallel prompting, the time to process  
778  $N$  queries is  $T_{\text{par}}(N)$ , so the parallel throughput is  $\frac{N}{T_{\text{par}}(N)}$ . The improvement is:  
779

780 
$$\Delta = \frac{N}{T_{\text{par}}(N)} - \frac{1}{T_{\text{seq}}}$$
  
781

782 Assuming  $T_{\text{par}}(N) = \frac{T_{\text{seq}}}{S(N)}$ , we substitute to get:  
783

784 
$$\Delta = \frac{N}{\frac{T_{\text{seq}}}{S(N)}} - \frac{1}{T_{\text{seq}}} = \frac{N \cdot S(N)}{T_{\text{seq}}} - \frac{1}{T_{\text{seq}}} = \frac{N \cdot S(N) - 1}{T_{\text{seq}}}$$
  
785

□

790 A.2 ASSUMPTIONS OF PROPOSITION 2  
791792 Let  $T_{\text{batch}} = T_{\text{setup}} + N \cdot T_{\text{MV}}$  be the wall-time for a batch (with matrix-vector attention), and  
793  $T_{\text{parallel}} = T_{\text{setup}} + T_{\text{MM}}$  for parallel prompting (with matrix-matrix attention). Then, the respective  
794 throughput values are:  
795

796 
$$\text{Throughput}_{\text{batch}} = \frac{N}{T_{\text{batch}}}, \quad \text{Throughput}_{\text{parallel}} = \frac{N}{T_{\text{parallel}}} \quad (9)$$
  
797

798 and  
799

800 
$$\frac{\text{Throughput}_{\text{parallel}}}{\text{Throughput}_{\text{batch}}} = \frac{T_{\text{batch}}}{T_{\text{parallel}}} = \frac{T_{\text{setup}} + NT_{\text{MV}}}{T_{\text{setup}} + T_{\text{MM}}} \quad (10)$$
  
801

802 where  $T_{\text{MV}}$  is per-query wall-time for the matrix-vector attentions, and  $T_{\text{MM}}$  is wall-time for the  
803 matrix-matrix product in the attention.  
804805 **Assumptions:**  
806807 

- The model and hardware support this masking and packing;  $T_{\text{MV}}$  and  $T_{\text{MM}}$  are measured  
808 compatibly.
- Time for setup is equal for standard batch processing and parallel prompting,  
809
- $N$  is small enough to avoid exceeding hardware or memory limits for both methods.

810 A.3 ASSUMPTIONS OF PROPOSITION 3  
811812 **Throughput Maximization** Let  $P$  be the parallel size (number of independent queries packed into  
813 a sequence for matrix-matrix attention),  $B$  the batch size (number of such sequences processed in  
814 parallel), and  $P \cdot B \leq S^*$  a hardware resource constraint (e.g., total token capacity).815 Let  $T_{\text{attn}}(P)$  denote the attention computation cost (function of  $P$ ), and  $T_{\text{mlp}}(B)$  denote the  
816 MLP/other backend (function of  $B$ ).817 Then, the throughput (queries per unit time) satisfies:  
818

819 
$$\text{Throughput}(P, B) = \frac{P \cdot B}{T_{\text{attn}}(P) + T_{\text{mlp}}(B)} \quad (11)$$
  
820  
821

822 and maximal throughput is achieved at  
823

824 
$$(P^*, B^*) = \arg \max_{P \cdot B \leq S^*} \frac{P \cdot B}{T_{\text{attn}}(P) + T_{\text{mlp}}(B)} \quad (12)$$
  
825

826 where  $T_{\text{attn}}(P)$  generally improves with  $P$  up to a hardware limit (then degrades), and  $T_{\text{mlp}}(B)$   
827 improves with  $B$  up to a limit.828 **Assumptions:**  
829830 

- $P$  queries packed per prompt,  $B$  prompts in a batch,  $PB \leq S^*$  (resource or hardware  
831 constraint).
- Model/hardware supports this arrangement;  $T_{\text{attn}}(P)$  and  $T_{\text{mlp}}(B)$  are the attention/MLP  
832 module wall times.
- $T_{\text{attn}}(P)$ ,  $T_{\text{mlp}}(B)$  are nonincreasing (improve) up to hardware limits, then nonmonotone.

  
833834 B TECHNICAL APPENDICES AND SUPPLEMENTARY MATERIAL  
835836 The decision to use different models and datasets for the analytical and ablation studies, as compared  
837 to the main downstream task evaluations, is motivated by both practical and scientific considerations.  
838 Large models like Llama 3-8B are computationally intensive, making it challenging to run extensive  
839 ablation and scaling experiments across a wide range of parameters. By using smaller models and  
840 synthetic datasets for these studies, we are able to systematically vary key factors (such as batch  
841 size, prefix length, and number of queries) and isolate the effects of our method in a controlled  
842 environment. This approach enables us to provide deeper insights into the scaling laws, bottlenecks,  
843 and generalization of our method, while reserving the large-scale, real-world benchmarks for the  
844 main results. We believe this combination offers a comprehensive and rigorous evaluation of our  
845 approach.  
846847 Table 1: Comparison of generation time and performance for downstream tasks with different methods  
848 on average of five times with Llama 3 8B model on A100-80G. Std denotes the across-run standard  
849 deviation of the time. F1 is computed as the harmonic mean of precision and recall in extractive QA.  
850851  
852 

| Method          | SQuAD   |      |       | QuAC    |      |       | DROP    |      |       |
|-----------------|---------|------|-------|---------|------|-------|---------|------|-------|
|                 | Time(s) | Std  | F1(%) | Time(s) | Std  | F1(%) | Time(s) | Std  | F1(%) |
| Standard        | 1277    | 0.08 | 87.2  | 3512    | 0.06 | 34.0  | 1330    | 0.08 | 58.1  |
| SeqBatch        | 566     | 0.21 | 84.2  | 386     | 0.10 | 29.1  | 1007    | 0.41 | 42.5  |
| Hydragen        | 1651    | 20.9 | 87.1  | 1230    | 6.74 | 34.0  | 471     | 3.85 | 58.2  |
| SGLang          | 337     | 0.49 | 87.4  | 854     | 0.17 | 32.7  | 377     | 0.56 | 58.5  |
| vLLM            | 369     | 0.46 | 87.4  | 889     | 0.57 | 32.8  | 413     | 0.44 | 58.5  |
| vLLM-RA         | 365     | 0.21 | 87.3  | 469     | 0.15 | 32.8  | 179     | 0.51 | 58.5  |
| <b>Parallel</b> | 167     | 0.16 | 87.2  | 243     | 0.32 | 33.9  | 110     | 0.09 | 58.1  |

861  
862 **Memory Usage** The observed increase in memory usage for the Parallel method on datasets results  
863 from dynamically maximizing batch sizes during inference. Our approach allows processing more

examples in a fixed memory footprint, improving throughput. To validate this, we reduced the maximum allowed batch size during inference on QuAC and observed a significant drop in memory usage, while still demonstrating substantial speedup over the baseline with the maximum possible batch size. For transparency, Table 3 lists the results across different batch size settings with our method. This demonstrates that our method flexibly trades off memory and throughput by adjusting batch size, and can achieve substantial speedup even at lower memory footprints.

Table 2: Comparison of memory usage with different methods with Llama 3 8B model on A100-80G.

| Dataset | Method   | Time(s) | Memory(GB) |
|---------|----------|---------|------------|
| SQuAD   | Standard | 590     | 55.7       |
|         | Parallel | 168     | 48.6       |
| QuAC    | Standard | 1799    | 55.0       |
|         | Parallel | 352     | 33.1       |
| DROP    | Standard | 654     | 54.3       |
|         | Parallel | 111     | 36.1       |

Table 3: QuAC: Inference Time and Memory Usage for Different Batch Sizes (Parallel Method)

| Batch Size | Inference Time (s) | Memory (GB) |
|------------|--------------------|-------------|
| Baseline   | 1799               | 55.0        |
| 8          | 872                | 16.9        |
| 16         | 677                | 19.8        |
| 32         | 420                | 24.7        |
| 64         | 352                | 33.1        |
| 128        | 342                | 54.0        |

**Effect of the Number of Questions.** We sweep over the number of queries for fixed document and query lengths. Table 4 shows that throughput improves as the number of parallel queries increases, particularly for larger models. At small batch sizes, non-attention operations dominate, but at large query counts, attention over long prefixes becomes the bottleneck—precisely where our parallel decoding provides the largest gains.

Table 4: Throughput (tokens/sec) under different batch sizes for parallel generation with CodeLlama-1B and CodeLlama-7B when  $doc\_len = 512$ ,  $q\_len = 12$ , and  $ans\_len = 5$ .

| Num Questions | Batch Size | Throughput-1B | Throughput-7B |
|---------------|------------|---------------|---------------|
| 128           | 1          | 4283          | 1931          |
|               | 2          | 4625          | 1843          |
|               | 4          | 3654          | 1468          |
|               | 8          | 2850          | 1018          |
| 256           | 1          | 5911          | 2115          |
|               | 2          | 6384          | 2250          |
|               | 4          | 5748          | 2071          |
|               | 8          | 4959          | 1615          |
| 512           | 1          | 5419          | 1850          |
|               | 2          | 6845          | 2214          |
|               | 4          | 7725          | 2382          |
|               | 8          | 7181          | 2146          |

**Sequence Length vs. Computation Gains Trade-off.** Both theory and empirical results confirm that throughput increases with batch/parallel size up to a point—after which the computational

918 overhead of longer input sequences (from packed prompts) outweighs the matrix-matrix compute  
 919 advantage. For example, on A100s, parallel sizes between 32 and 64 are optimal for typical workloads.  
 920

921 **Compatibility with Speculative Decoding.** Parallel Prompting (fanning out multiple suffixes at  
 922 lock-step) is designed for simultaneous multi-query generation, while speculative decoding focuses on  
 923 verifying a single sequence. These are distinct but potentially complementary: speculative decoding  
 924 could be performed within each branch created by Parallel Prompting, or adapted to verify multiple  
 925 shared-prefix continuations in parallel.

926 **Developer Overhead and Practical Adoption.** In many production stacks, the shared-prefix bound-  
 927 ary is already explicit: for example, retrieval-augmented generation (RAG) pipelines concatenate  
 928 retrieved context (prefix) with a question (suffix), and batched APIs naturally group queries under a  
 929 common header or instruction. In these settings, enabling Parallel Prompting requires only providing:  
 930 (1) the token span (or delimiter) for the shared prefix, and (2) a list of per-query suffixes. This makes  
 931 practical adoption straightforward in most modern LLM serving pipelines.

932 **Memory Scaling Experiments** To systematically study memory and throughput scaling, we  
 933 conducted experiments varying shared prefix length (128, 256, 512, 1024 tokens), output length (5  
 934 vs 100 tokens), number of unique prefixes (num\_doc: 4 vs 8), and number of questions per prefix  
 935 (num\_q: 32, 64, 128). Our results reveal several key patterns: (1) Output length is the dominant  
 936 driver of memory usage, followed by num\_doc and context length, with num\_q having a smaller but  
 937 non-negligible effect. (2) Long outputs dominate memory via KV cache growth across all decode  
 938 steps. (3) num\_doc has a much larger impact when output is long, as a longer context is carried  
 939 through every generated token. (4) Longer shared prefixes add memory, but the effect is modest  
 940 compared to output length and num\_doc, consistent with effective prefix sharing across the batch.

942 Table 5: Memory Usage (MB) and Throughput (tokens/s) for Output Length 100  
 943

| 945 <b>Prefix</b> | <b>num_doc</b> | <b>num_q</b> | <b>Memory (MB)</b> | <b>Throughput (tok/s)</b> |
|-------------------|----------------|--------------|--------------------|---------------------------|
| 946 128           | 4              | 32           | 7031               | 4490                      |
| 947 128           | 8              | 32           | 15814              | 5286                      |
| 948 128           | 4              | 64           | 20104              | 4825                      |
| 949 128           | 8              | 64           | 28617              | 2868                      |
| 950 128           | 4              | 128          | 37509              | 3704                      |
| 951 128           | 8              | 128          | 54429              | 2810                      |
| 952 256           | 4              | 32           | 7131               | 4540                      |
| 953 256           | 8              | 32           | 16109              | 5231                      |
| 954 256           | 4              | 64           | 20399              | 4624                      |
| 955 256           | 8              | 64           | 28927              | 2834                      |
| 956 256           | 4              | 128          | 37829              | 3705                      |
| 957 256           | 8              | 128          | 54761              | 2780                      |
| 958 512           | 4              | 32           | 7333               | 4462                      |
| 959 512           | 8              | 32           | 16689              | 4852                      |
| 960 512           | 4              | 64           | 20968              | 4627                      |
| 961 512           | 8              | 64           | 29545              | 2752                      |
| 962 512           | 4              | 128          | 38472              | 3692                      |
| 963 512           | 8              | 128          | 55433              | 2747                      |
| 964 1024          | 4              | 32           | 7766               | 4289                      |
| 965 1024          | 8              | 32           | 17932              | 4217                      |
| 966 1024          | 4              | 64           | 22174              | 4262                      |
| 967 1024          | 8              | 64           | 30787              | 2639                      |
| 968 1024          | 4              | 128          | 39751              | 3792                      |
| 969 1024          | 8              | 128          | 56787              | 2559                      |

970 **Effect of Model Size** The performance of LLM’s generation can be affected by various factors such  
 971 as number of queries, batch size and the length of prefixes. We also run experiments with various

972  
973  
974 Table 6: Memory Usage (MB) and Throughput (tokens/s) for Output Length 5 tokens  
975  
976  
977  
978  
979  
980  
981  
982  
983  
984  
985  
986  
987  
988  
989  
990  
991  
992  
993  
994  
995  
996  
997

| Prefix Length | Num_Documents | Num_Questions | Memory (MB) | Throughput (tok/s) |
|---------------|---------------|---------------|-------------|--------------------|
| 128           | 4             | 32            | 3187        | 2144               |
| 128           | 8             | 32            | 4324        | 6794               |
| 128           | 4             | 64            | 4798        | 7412               |
| 128           | 8             | 64            | 5767        | 9700               |
| 128           | 4             | 128           | 6735        | 9060               |
| 128           | 8             | 128           | 8724        | 9602               |
| 256           | 4             | 32            | 3290        | 1875               |
| 256           | 8             | 32            | 4622        | 5605               |
| 256           | 4             | 64            | 5095        | 7264               |
| 256           | 8             | 64            | 6073        | 8928               |
| 256           | 4             | 128           | 7039        | 8627               |
| 256           | 8             | 128           | 9041        | 9304               |
| 512           | 4             | 32            | 3512        | 1976               |
| 512           | 8             | 32            | 5260        | 5098               |
| 512           | 4             | 64            | 5687        | 6479               |
| 512           | 8             | 64            | 6684        | 7472               |
| 512           | 4             | 128           | 7671        | 7831               |
| 512           | 8             | 128           | 9727        | 8520               |
| 1024          | 4             | 32            | 4143        | 1573               |
| 1024          | 8             | 32            | 6906        | 3601               |
| 1024          | 4             | 64            | 7135        | 4882               |
| 1024          | 8             | 64            | 8426        | 5404               |
| 1024          | 4             | 128           | 9261        | 6282               |
| 1024          | 8             | 128           | 11751       | 6689               |

998  
9991000 configurations with CodeLlama-7b-Inst (Rozière et al., 2024) and Sheared-LLaMA-1.3B (Xia et al.,  
1001 2024) since different model sizes could also affect generation performance. See Table 7 for results.

1002

1003 Table 7: Comparing the throughput using parallel Batching with 7B and 1B Llama model with  
1004 different lengths of doc length when  $q\_len = 12 \parallel q\_num = 128 \parallel ans\_len = 5$  and the number  
1005 of unique doc content equals 8. As the content length increases, the degradation of throughput  
1006 performance becomes severe.

1007

| doc.len | Throughput(1B)(tokens/second) | Throughput(7B)(tokens/second) |
|---------|-------------------------------|-------------------------------|
| 256     | 9512                          | 2750                          |
| 512     | 8199                          | 2430                          |
| 1024    | 6591                          | 1924                          |

1011

1012

1013

1014

1015

1016

1017

1018

1019

1020

1021

1022

1023

1024

1025